ARTICLE

Channel-Resolved Ultrafast Dissociation Dynamics of NO_2 Molecules Studied via Femtosecond Time-Resolved Ion Imaging

Qin-xin Wang[a,b*], Dan-dan Shi[a], Jun-feng Zhang[a], Xue Wang[a], Yu Si[a], Chun-bin Gao[a], Jian Fang[a], Si-zuo Luo[b*]

a. College of Electrical Engineering, Jilin Engineering Normal University, Changchun 130012, China
b. Institute of Atomic and Molecular Physics and Jilin Provincial Key Laboratory of Applied Atomic and Molecular Spectroscopy, Jilin University, Changchun 130012, China

(Dated: Received on July 26, 2018; Accepted on September 20, 2018)

The ultrafast dissociation dynamics of NO_2 molecules was investigated by femtosecond laser pump-probe mass spectra and ion images. The results show that the kinetic energy release of NO^+ ions has two components, 0.05 eV and 0.25 eV, and the possible dissociation channels have been assigned. The channel resolved transient measurement of NO^+ provides a method to disentangle the contribution of ultrafast dissociation pathways, and the transient curves of NO^+ ions at different kinetic energy release are fitted by a biexponential function. The fast component with a decay time of 0.25 ps is generated from the evolution of Rydberg states. The slow component is generated from two competitive channels, one of the channel is absorbing one 400 nm photon to the excited state A^2B_2, which has a decay time of 30.0 ps, and the other slow channel is absorbing three 400 nm photons to valence type Rydberg states which have a decay time less than 7.2 ps. The channel and time resolved experiment present the potential of sorting out the complex ultrafast dissociation dynamics of molecules.

Key words: Ultrafast dynamics, Strong field ionization, Photodissociation dynamic, Velocity map imaging

I. INTRODUCTION

The ultrafast dynamics of NO_2 has attracted particular interest, due to its importance for understanding the photodissociation of polyatomic molecules [1−8]. Femtosecond time-resolved investigations of NO_2 have been performed to study the transient behaviors of excited states and to disentangle the dissociation mechanisms in recent years, such as dissociative ionization [9, 10], excited-state dynamics [11−17], and conical intersection [1, 18, 19]. López-Martens *et al.* studied ultrafast dissociation dynamics of NO_2 using femtosecond laser pump-probe fluorescence depletion spectroscopy [13], and found that the dominant dissociation occurred through the excited state populated by absorbing three 400 nm photons, with a decay time shorter than 600 fs. Eppink *et al.* studied the ultrafast dissociation of NO_2 using femtosecond time-resolved ion imaging method, and the fragment NO^+ with a kinetic energy of 0.28 eV was observed, which corresponded to the dissociative ionization channel of absorbing three 400 nm photons to Rydberg states and absorbing another 266 nm photon to ionization [14]. The transient curve of NO^+ has two kinds of decay time, with the fast decay time of (90±10) fs and the slow one of (4000±400) fs; the fast channel corresponds to dissociation from Rydberg state and the slow channel is from excited state A^2B_2. Form *et al.* observed the oscillation of ion signal from slow decay channel, and they assigned the oscillation to the roaming of O atom in the excited states [15]. While Irimia *et al.* assigned the oscillation to the superposition of oscillating wavepacket between Rydberg and valence character of predissociation states [16]. The ultrafast dissociation dynamics of NO_2 such as the relation between oscillation of ion and wavepacket motion is still a hot debated topic, which has attracted a lot of attention recently [16−20]. Vredenborg *et al.* studied the multiphoton multichannel dissociation dynamics of NO_2 by time-resolved coincident imaging, the contribution of different excited states and dissociation channels have been identified [17]. They found that the dissociation occurring at short delay time (<300 fs) comes from a repulsive potential energy surface, which is populated by absorbing three 400 nm photons, and this Rydberg state can transfer to dissociation states via conical intersection. The ions from the slow delay channel are generated from either a Rydberg state or excited state A^2B_2, this Rydberg state is populated by absorbing three 400 nm photons, and the A^2B_2 state is populated by absorbing one 400 nm photon. These previous experiments present very different decay channels and decay

*Authors to whom correspondence should be addressed. E-mail: wangqinxin_2006@126.com, luosz@jlu.edu.cn

time because of the multiple excitation states involved during the ultrafast dissociation of NO_2 [11, 14−18]. It will be interesting to provide a further discussion on channel resolved ultrafast dissociation dynamics of NO_2 in strong laser fields [21].

In this work, we perform an experimental study on ultrafast dissociation dynamics of NO_2 by using two-color femtosecond laser (400 nm+800 nm) pump-probe method with velocity map imaging (VMI) measurement. The obtained kinetic energy release (KER) spectra of NO^+ have two components, one component with kinetic energy of 0.05 eV and the other with kinetic energy of 0.25 eV. The dissociation channels have been identified and the transient behaviors of $NO_2{}^+$ and NO^+ have been discussed by combining the measurement of the transient curves of mass spectra and channel-resolved transient evolutions of NO^+ ion images.

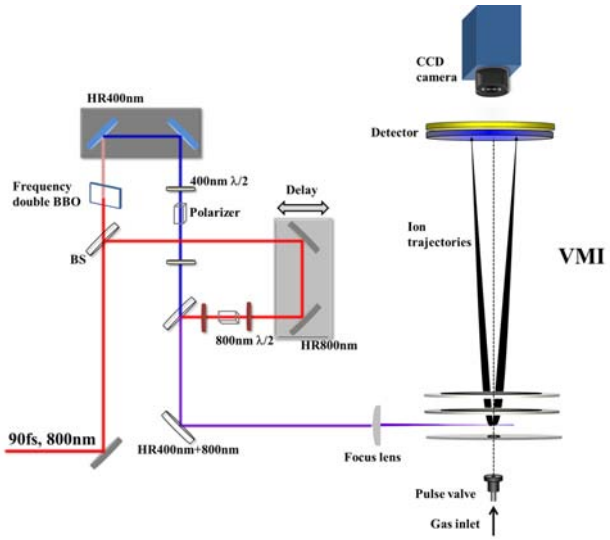

FIG. 1 Schematic of the experimental setup used to induce and monitor ultrafast dynamics of molecules.

II. EXPERIMENTS

A schematic drawing of experimental setup used in the present study is shown in FIG. 1. A chirped pulse amplified (CPA) Ti:sapphire laser is employed to produce a 90 fs, 800 nm linearly polarized laser beam with a repetition rate of 10 Hz. A Mach-Zehnder interferometer is used to split the laser beam into two parts with a variable delay for a pump-probe measurement. The intensity of each beam varies by using a half-wave plate and a Glan polarizer. The pump laser is frequency-doubled to 400 nm through a 0.5 mm BBO crystal and the polarization is rotated by a half-wave ($\lambda/2$) plate. The probe laser beam is sent through a computer-controlled delay stage to change the delay time between the pump and probe laser beams. The pump and probe laser intensities are 15 and 100 μJ, respectively. The pump and probe laser beams are collinearly focused onto a supersonic molecular beam in a detection chamber by a 250-mm-focal-length lens. The zero delay time of pump and probe laser beams is determined by measuring the cross correlation of Xe^+, in which the FWHM of cross correlation spectrum is 143 fs from Gaussian fitting. This molecular beam is produced by expanding 2% NO_2 seeded in helium with a stagnation pressure of 2 bars through a 0.5-mm orifice of a pulsed valve. There might be some N_2O_4 molecules coexisting in the molecular beam because of its high equilibrium constant. However, this does not affect measurements because the absorption of NO_2 dominates at 400 nm. We also check the contribution of $NO_2{}^+$ from ionization of NO_2 and dissociation ionization of N_2O_4 by measuring the ion images of $NO_2{}^+$, we find $NO_2{}^+$ dominates the species generated from the ionization of NO_2 since the ionization energy of NO_2 (9.6 eV) is much smaller than that of N_2O_4 (11.4 eV). So the influence of N_2O_4 on transient behaviors of NO^+ can be neglected in this work. The measurement is carried out in a velocity map imaging system based on the design of Eppink and Parker [22]. The microchannel plate is gated by applying a 300-ns voltage pulse at the specific delay time to select imaging of fragment NO^+ ion. Images of the ion signal on the phosphor screen of the detector are recorded using a CCD camera. The mass spectra are obtained through monitoring the phosphor screen by a photomultiplier tube, which are accumulated and averaged by a digital storage oscilloscope.

III. RESULTS AND DISCUSSION

Multiphoton absorption of pump and probe lasers will lead to both ionization and dissociation of NO_2 molecules. For convenience, a schematic representation of the relevant energy levels of NO_2, $NO_2{}^+$ [17, 18, 22−24] is shown in FIG. 2(a). We label the various possible dissociation channels with (1)−(5). The photoabsorption cross section curve extracted from Ref.[25] is shown in FIG. 2(b), and two arrows point to the absorption position of one and three 400 nm photons.

In the experiment, we use a weak pump laser (400 nm) to excite molecules only and no ion signals of $NO_2{}^+$ or NO^+ are observed when pump laser interacts with molecules. One and three photons excitation processes coexist when we carefully choose the pump laser intensity. The intense probe laser (800 nm) has been used to make sure all the excitation states are dissociated and ionized. The mass spectra of NO_2 obtained in the pump-probe experiment at different delay time are shown in FIG. 3. The mass spectra shown in FIG. 3(a) is produced at negative delay time and only weak $NO_2{}^+$ and NO^+ signals are observed, these signals are generated from interacting with probe laser only. The enhancement of both $NO_2{}^+$ and NO^+ signals

DOI:10.1063/1674-0068/cjcp1807177

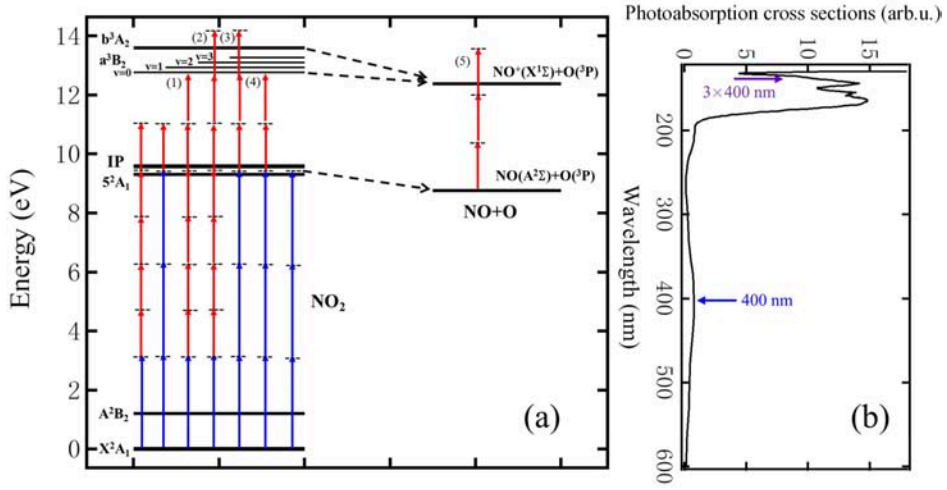

FIG. 2 (a) Energy levels of NO_2 and NO_2^+ and the dissociation and ionization channels. A 400 nm photon is represented by blue arrows and an 800 nm photon is represented by red arrows. Different dissociation channels are represented by (1)−(5). (b) Photoabsorption cross section curves are extracted from Ref.[24], two arrows point to the absorption of one and three 400 nm photons, respectively.

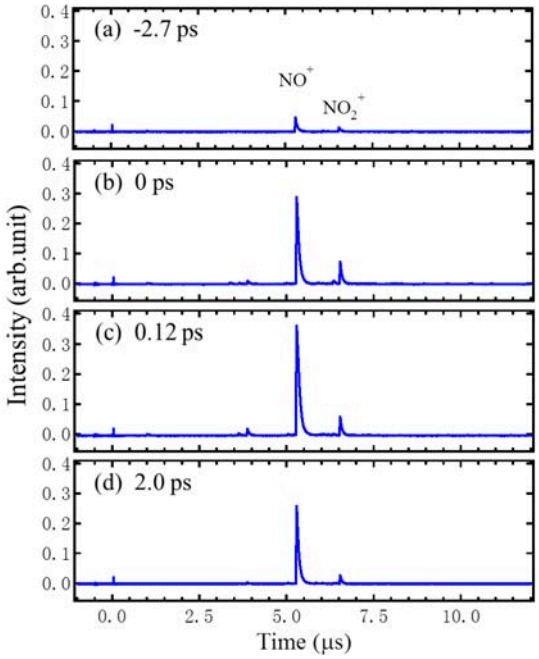

FIG. 3 Time of flight mass spectra obtained at different delay time. The energies of the pump and probe pulses are 15 and 100 μJ, respectively.

are observed and the intensity of the NO^+ is four times larger than that of NO_2^+ at zero delay time as shown in FIG. 3(b). The mass spectra obtained at delay time of 0.12 ps and 2.0 ps are shown in FIG. 3 (c) and (d). The signal of NO_2^+ is very weak at delay time of 2.0 ps. Comparing the mass spectra obtained at different delay time, it is obvious to see that the decrease of NO_2^+ signal is much faster than NO^+ signal and the maximum signal of NO_2^+ is smaller than that of NO^+.

The pump-probe transient curves of ultrafast dissociation and ionization of NO_2 molecules are shown in FIG. 4. The transient curve of NO_2^+ is shown in FIG. 4(a), with the signal increasing rapidly around the zero delay time, after that the signal decreases very fast. For the direct ionization, NO_2^+ could be produced from different channels, such as absorbing one 400 nm photon to excited state A^2B_2 followed by absorbing five 800 nm photons to ionization, or absorbing three 400 nm photons to excited Rydberg state followed by absorbing one 800 nm photon to ionization. We can also see that the maximum signals of NO_2^+ and NO^+ appear at different delay time, 0.11 ps and 0.23 ps respectively, and the signal of NO^+ increases as the signal of NO_2^+ decreases with comparable time of 0.12 ps. This observation and different evolution of NO_2^+ and NO^+ imply that most of the NO_2 population is lost through a dissociative ionization route [14]. From the measured transient curves, the time-dependent signal intensity $S(t)$ is analyzed using a least-squares fitting program, which is given by [26]

$$S(t) = \sum_i c_i \sigma \exp\left[\left(\frac{\sigma}{2\tau_i}\right)^2 - \frac{t}{\tau_i}\right]\left[1 - \mathrm{erf}\left(\frac{\sigma}{2\tau_i} - \frac{t}{\sigma}\right)\right]$$

where c_i is the amplitude of the component, τ_i is the decay time and σ is related to the FWHM of the excitation laser pulse. In this way, a single decay time of (0.28±0.05) ps is used to fit the NO_2^+ curve, and two decay time of (0.25±0.05) ps and (13.0±1.0) ps are used to perform a best fitting of the NO^+ curve, these two exponential components (see FIG. 4(b)) are generated from the fast and slow dissociation channels of NO_2.

The KER spectra of NO^+ generated from dissociative

DOI:10.1063/1674-0068/cjcp1807177

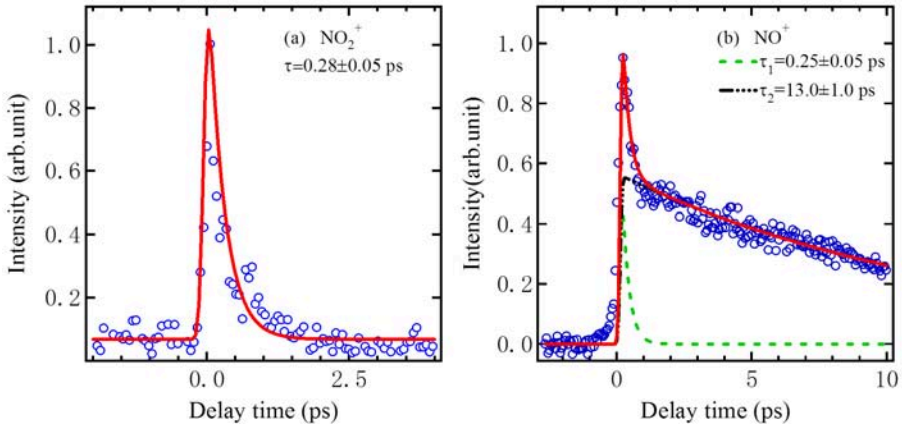

FIG. 4 The transient curves of NO_2^+ and NO^+ as well as their best fitting results, and blue circles and red line represent experimental and fitting results. (a) The decay time of the NO_2^+ is (0.28±0.05) ps, (b) the decay time of the NO^+ transient curve fitted by a biexponential function is (0.25±0.05) ps and (13.0±1.0) ps.

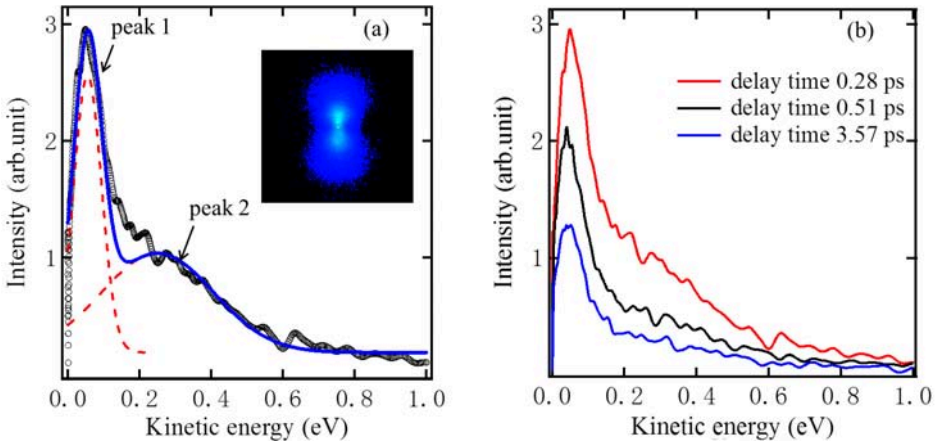

FIG. 5 The kinetic energy release spectra obtained by Abel inversion of the ion images. (a) The kinetic energy release of NO^+ at 0.28 ps. The inset picture is raw image of NO^+. Two peaks at kinetic energy of 0.05 and 0.25 eV fit the kinetic energy release spectrum. (b) The kinetic energy release spectra of NO^+ ions at different delay time.

ionization of NO_2 at different pump-probe delay time are shown in FIG. 5. The velocity image obtained at delay time of 0.28 ps shows two ion distribution parts and the KER distribution can be fitted by two Gaussian functions, as shown in FIG. 5(a), giving a value of 0.05 eV for the inner part ions and 0.25 eV for the outer part ions. The comparison of measured KER from different groups [14, 15, 17] (using 400 nm pump and 266 nm probe) is shown in Table I. Our measured KERs of NO^+ are in agreement with previous experimental results, which indicates all the dissociation channels after pump by 400 nm laser have been observed. The contribution of fast and slow decay channels to different KER distributions of NO^+ is also presented in Table I. The comparison of KER spectra at different delay time between pump and probe lasers is shown in FIG. 5(b), the intensities of KER spectra change as the delay time increases.

The measured KER spectra of ions provide information on analysis of the dissociation of NO_2 in two-color lasers. NO^+ can be produced from dissociation channels (1)−(5) as shown in FIG. 2. In channel (1), NO_2 first absorbs one 400 nm photon and is populated to a long-life A^2B_2 state [13−15], then absorbs six 800 nm photons to a^3B_2 state with appearing potential of 12.38 eV, and dissociates to NO^++O [23]. In this case, the energy obtained by multi-photon absorption is 12.5 eV when the bandwidth of our laser is considered, the release energy for dissociation channel (1) is 0.12 eV. This release energy is shared by NO^+ and O. According to the law of momentum conservation between two fragments generated from dissociation, the KER of fragment NO^+ from one particular channel can be calculated from the total release energy by

$$E_{\mathrm{kin,NO^+}} = \frac{m_{\mathrm{O}}}{m_{\mathrm{NO_2}}} E_{\mathrm{kin,tot}} \quad (1)$$

DOI:10.1063/1674-0068/cjcp1807177

TABLE I The KERs of NO^+ come from dissociative ionization of NO_2.

Dissociate channels	KER/eV			
	This work	Eppink *et al.* [14]	Form *et al.* [15]	Vredenborg *et al.* [17]
Low kinetic energy	0.05	0.015[a]	0.01[a]	0.00, 0.10[a]
High kinetic energy	0.25	0.28[b]	0.31[a], 0.31[b]	0.24[a], 0.38[b]

[a] Kinetic energy from slow decay channel.
[b] Kinetic energy from fast decay channel.

where $E_{\text{kin, NO}^+}$ is the kinetic energy of the fragment NO^+, m_O and m_{NO} are the mass of O and NO_2, $E_{\text{kin,tot}}$ is the total kinetic energy. It leads to a KER of NO^+ around 0.04 eV from channel (1), which agrees with our observation of low KER value at 0.05 eV. The low KER ions can also be generated from channel (4), which is produced from two-photon dissociation from a short life time Rydberg state after absorbing three 400 nm photons. In this channel, the final excess energy of the fragment ions $NO^+(X^1\Sigma)$+$O(^3P)$ is the same as channel (1). The NO^+ ions with high KER (0.25 eV) can be assigned to the dissociation from three channels, *i.e.*, channels (2), (3) and (5) according to the relevant energy levels shown in FIG. 2. In the channel (2), NO_2 first absorbs one 400 nm photon to long life state A^2B_2 and then absorbs another seven 800 nm photons to ionization, after that the molecular ion is populated at ionic states a^3B_2 and b^3A_2 which will dissociate to $NO^+(X^1\Sigma)$+$O(^3P)$. The appearance energy of these two fragments is 12.38 eV, and NO^+ is dissociated from different vibration state (v=0, 1, 2, 3) of both ionic states. The obtained KERs of NO^+ are 0.13, 0.2, 0.25, and 0.31 eV when dissociation occurs from vibration states of a^3B_2 and the KER of ion is 0.42 eV after dissociation occurs from b^3A_2 state. The KERs of NO^+ generated from these channels agree well with the measured results which have a broad distribution around 0.25 eV (from 0.0 eV to 0.50 eV). For the dissociation channel (3), NO_2 first absorbs three 400 nm photons to a short life Rydberg state and absorbs another three 800 nm photons to a^3B_2 and b^3A_2 ionic states [15, 16]. For the dissociation channel (5), NO_2 first absorbs three 400 nm photons to a long life Rydberg state 5^2A_1 or 6^2A_1 [16]. The 5^2A_1 state correlates to the $3^2\Sigma_g^+$(3d) Rydberg state at linear geometry, and the 6^2A_1 state correlates to the $1^2\Delta_g$(3d) Rydberg state at linear geometry. These linear geometry Rydberg states are crossed by two dissociative states which can dissociate to $NO(A^2\Sigma)$+$O(^3P)$, the $NO(A^2\Sigma)$ can be ionized by absorbing another three 800 nm photons. The appearance energy of $NO(A^2\Sigma)$+$O(^3P)$ is 8.75 eV [17, 18, 23] and the energy of three 400 nm photons is 9.3 eV, so the obtained KER of NO^+ from this channel is 0.19 eV.

The channel resolved transient behavior of NO^+ ions illuminates light on the ultrafast dissociation process of NO_2 molecules, and provides an opportunity to disentangle the contribution of fast and slow dissociation pathways. The transient curves of NO^+ with KER at 0.05 and 0.25 eV are shown in FIG. 6, the red circles are the signal intensity of ions from selected KER distribution and red lines are the best fitting curves using biexponential function. It is clear to see that all of three transient curves are fitted by a fast decay curve (green dash line) and a slow decay curve (black dash dot line). The transient curve of low KER NO^+ ions (0.05 eV) is shown in FIG. 6(a) with the fast decay time of (0.22±0.05) ps and the slow decay time of (30.0±3.0) ps. The transient curve for high KER NO^+ ions (0.25 eV) is shown in FIG. 6(b) with the fast and slow decay time of (0.14±0.06) ps and (7.2±2.0) ps. The transient curve of all detected NO^+ ions is shown in FIG. 6(c), and the decay time are (0.19±0.05) ps and (11.0±2.0) ps, these values agree with the measurement

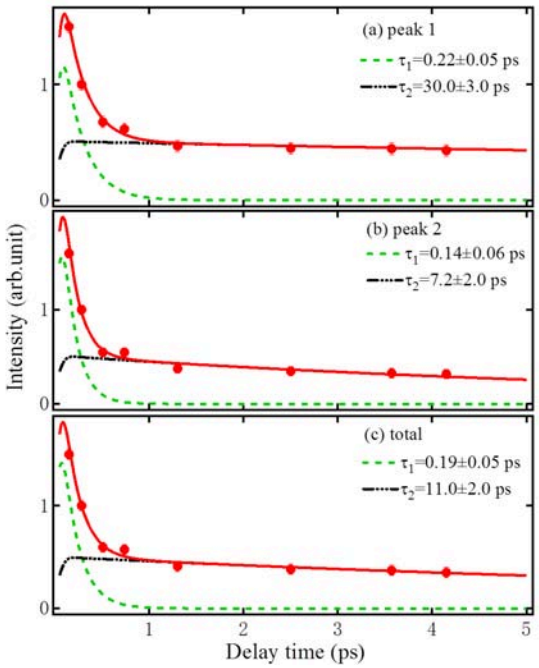

FIG. 6 The transient curves of different channels, the red circles are the intensity of specific channel at different delay time from experiment and red lines are the fitting. (a) The transient curve of low KER channel (0.05 eV), (b) the transient curve of high KER channel (0.25 eV), and (c) the transient curve of all channels in ion images.

DOI:10.1063/1674-0068/cjcp1807177

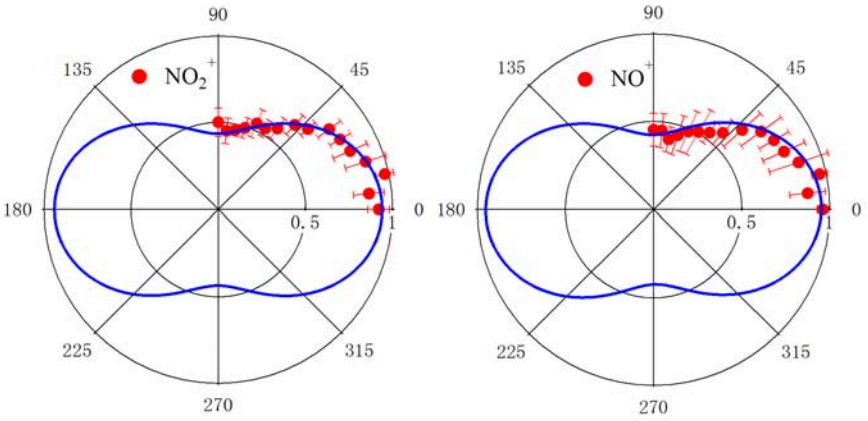

FIG. 7 Angular distributions of NO_2^+ and NO^+ ions at pump probe delay time of 0.28 ps. The blue lines are from the fitting using Legendre polynomials $I=1+\sum \beta_{2i}P_{2i}$.

obtained from transient curve of mass spectra as shown in FIG. 4(b). The fast decay time of different KER ions is close to each other while the decay time of slow component is different from each other (30.0±3.0) ps for low KER ions and (7.2±2.0) ps for high KER ions, which means the fast decay channels for low and high KER ions are from the same excitation state and slow decay channels for low and high KER ions are dissociated from different excitation states. The fast decay channels are generated by absorbing three 400 nm photons to Rydberg state and absorbing another two or three 800 nm photons to dissociation. Comparing the analysis of previous studies [15−17] with the above analysis of KER distributions from different dissociation channels, the low KER ions with slow decay time shown in FIG. 6(a) are generated from long life A^2B_2 state, the high KER ions with slow decay time as shown in FIG. 6(b) can both be dissociated from A^2B_2 state and 5^2A_1 or 6^2A_1 excitation states. The life time of A^2B_2 state is (30.0±3.0) ps under our laser condition, which is close to the measurement result of Stolyarov *et al.* [27]. The high KER ions are more likely generated from dissociation channel (5) than channel (2) under our experiment condition. The channel (5) occurs by absorbing three 400 nm photons and being excited to 5^2A_1 or 6^2A_1 states with a life time less than (7.2±2.0) ps. It is important to notice that Form *et al.* also observed a slow decay for the low KER NO^+ ions, and a slow decay and a fast decay for high KER component of NO^+ ions [15], but they did not observe dissociation channel (4) in the experiment because they used 266 nm laser as a probe. Using the intense laser with wavelength centered at 800 nm as a probe can provide more information on ultrafast dissociation dynamics of different molecular excited states. It is noteworthy that the decay time of slow component relays on the contribution of excited state A^2B_2 and Rydberg state 5^2A_1 or 6^2A_1, and the contributions of different states can be controlled by changing the laser intensity [21]. At low laser intensity, the channel with the one photon excited state A^2B_2 dominates, and as the laser intensity increases, the process involved in three-photon excitation to 5^2A_1 or 6^2A_1 will have important contribution. The difference of decay time measured from different experiments can be attributed to the different intensity of pump laser [11, 14−18, 21], so specific states can be selectively excited to by carefully choosing the intensity of pump laser.

The angular distributions of NO_2^+ and NO^+ obtained from measuring the signal intensities at different angles between pump and probe laser at delay time of 0.28 ps are shown in FIG. 7. These angular distributions show a maximum at θ=0° and a minima at θ=90°, which are fitted by an expansion of Legendre polynomials $I=1+\sum \beta_{2i}P_{2i}$ (β_2=0.168 and 0.177 for NO_2^+ and NO^+ respectively). The anisotropic of angular distribution is affected by the transition moment between ground and excited states, and is also influenced by the shape of the orbital from which an electron is removed. When intense laser interacts with excited NO_2 molecules, the angular distributions of NO_2^+ and NO^+ contain the information of molecular excited orbital and neutral-ionic state correlation [28, 29]. In the present experiment, the same angular distributions of NO_2^+ and NO^+ demonstrate that the parent ion and fragment ion are produced from ionization of the same excited states at the delay time of 0.28 ps. Strong field dissociative ionization is a powerful method to detect the ultrafast molecular dynamics, which can provide plenty of information on ultrafast dynamics of excitation states [28−30].

IV. CONCLUSION

The ultrafast dissociation dynamics of NO_2 in two-color femtosecond laser has been studied by measuring the time-resolved mass spectra and ion images, the re-

DOI:10.1063/1674-0068/cjcp1807177

sults demonstrate that the pump-probe transient evolution of NO^+ is generated from three ultrafast dissociation channels. The NO^+ generated from fast decay channels has KER peaks at 0.05 eV and 0.25 eV, which are generated by absorbing three 400 nm photons to Rydberg state and absorbing another two or three 800 nm photons to dissociation, and the lifetime of fast decay channel is (0.25±0.05) ps. The NO^+ generated from slow decay channel has two KER components, the low KER ions are produced form multi-photon dissociation of A^2B_2 state and have a life time of (30.0±3.0) ps, and the high KER ions are produced from absorbing three 400 nm photons to Rydberg predissociation state, with a lifetime of less than (7.2±2.0) ps.

V. ACKNOWLEDGMENTS

This work was supported by the National Natural Science Foundation of China (No.11704148, No.11847039, No.11534004).

[1] H. J. Wörner, J. B. Bertrand, B. Fabre, J. Higuet, H. Ruf, A. Dubrouil, and S. Patchkovskii, Science **334**, 208 (2011).
[2] S. M. Poullain, C. Elkharrat, W. B. Li, K. Veyrinas, J. C. Houver, C. Cornaggia, T. N. Rescigno, R. R. Lucchese, and D. Dowek, J. Phys. B: At. Mol. Opt. Phys. **47**, 124024 (2014).
[3] T. Suzuki, J. Phys. B: At. Mol. Opt. Phys. **47**, 124001 (2014).
[4] D. D. Zhang, Q. Ni, S. Z. Luo, J. Zhang, H. Liu, H. F. Xu, M. X. Jin, and D. J. Ding, Chin. Phys. Lett. **28**, 033301 (2011).
[5] D. Strasser, L. H. Haber, B. Doughty, and S. R. Leone, Mol. Phys. **106**, 275 (2008).
[6] D. D. Zhang, Z. Fan, E. P. Sun, J. F. Zhang, H. Liu, H. F. Xu, M. X. Jin, and D. J. Ding, Chin. Sci. Bull. **56**, 855 (2011).
[7] A. Stolow, Int. Rev. Phys. Chem. **22**, 377 (2003).
[8] A. Tehlar and H. J. Wörner, Mol. Phys. **111**, 2057 (2013).
[9] I. Wilkinson, I. A. Garcia, B. J. Whitaker, J. B. Hamar, and V. Blanchet, Phys. Chem. Chem. Phys. **12**, 15766 (2010).
[10] K. Vijayalakshmi, C. P. Safavan, G. Ravindra Kumar, and D. Mathur, Chem. Phys. Lett. **207**, 37 (1997).
[11] J. A. Davies, R. E. Continetti, D. W. Chandler, and C. C. Hayden, Phys. Rev. Lett. **84**, 5983 (2000).
[12] J. A. Davies, J. E. LeClaire, R. E. Continetti, and C. C. Hayden, J. Chem. Phys. **111**, 1 (1999).
[13] R. B. López-Martens, T. W. Schmidt, and G. Roberts, J. Chem. Phys. **111**, 7183 (1999).
[14] A. T. J. B. Eppink, B. J. Whitaker, E. Gloaguen, B. Soep, A. M. Coroiu, and D. H. Parker, J. Chem. Phys. **121**, 7776 (2004).
[15] N. T. Form, B. J. Whitaker, L. Poissonand, and B. Soep, Phys. Chem. Chem. Phys. **8**, 2925 (2006).
[16] D.Irimia, I. D. Petsalakis, G. Theodorakopoulos, and M. H. M. Janssen, J. Phys. Chem. A **114**, 3157 (2010).
[17] A. Vredenborg, W. G. Roeterdink, and M. H. M. Janssen, J. Chem. Phys. **128**, 204311 (2008).
[18] B. Liu, J. Zhu, B. Wang, Y. Wang, and L. Wang, J. Phys. Chem. A **113**, 13839 (2009).
[19] Y. Arasaki, K. Takatsuka, K. Wang, and V. McKoy, J. Chem. Phys. **132**, 124307 (2010).
[20] J. B. Hamard, R. Cireasa, B. Chatel, V. Blanchet, and B. J. Whitaker, J. Phys. Chem. A **114**, 3167 (2010).
[21] R. Forbes, A. E. Boguslavskiy, I. Wilkinson, J. G. Underwood, and A. Stolow, J. Chem. Phys. **147**, 054305 (2017).
[22] A. T. J. B. Eppink and D. H. Parker, Rev. Sci. Instrum. **68**, 3477 (1997).
[23] I. Wilkinson and B. J. Whitaker, Annu. Rep. Prog. Chem. Sect. C **106**, 274 (2010).
[24] P. Baltzer, L. Karlsson, B. Wannberg, D. M. P. Holland, M. A. MacDonald, M. A. Hayes, and J. H. D. Eland, Chem. Phys. **237**, 451 (1998).
[25] J. W. Au and C. E. Brion, Chem. Phys. **218**, 109 (1997).
[26] T. Fiebig, M. Chachisvilis, M. Manger, A. H. Zewail, A. Douhal, I. Garcia-Ochoa, and A. de La HozAyuso, J. Phys. Chem. A **103**, 7419 (1999).
[27] D. Stolyarov, E. Polyakova, I. Bezel, and C. Wittig, Chem. Phys. Lett. **358**, 71 (2002).
[28] M. Kotur, C. Zhou, S. Matsika, S. Patchkovskii, M. Spanner, and T. C. Weinacht, Phys. Rev. Lett. **109**, 203007 (2012).
[29] M. Kotur, T. C. Weinacht, C. Zhou, and S. Matsika, Phys. Rev. X **1**, 021010 (2011).
[30] S. Matsika, M. Spanner, M. Kotur, and T. C. Weinacht, J. Phys. Chem. A **117**, 12796 (2013).

DOI:10.1063/1674-0068/cjcp1807177